

# INDOOR ROBOT NAVIGATION USING LOG-POLAR LOCAL MAPS

L. Longega \* S. Panzieri \* F. Pascucci \*\* G. Ulivi \*

\* *Dipartimento di Informatica e Automazione  
Università di Roma Tre  
Via della Vasca Navale 79, 00146 Roma, Italy  
{longega, panzieri, ulivi}@dia.uniroma3.it*

\*\* *Dipartimento di Informatica e Sistemistica  
Università La Sapienza  
Via Eudossiana, 18, 00184 Roma, Italy  
{pascucci}@dia.uniroma3.it*

Abstract: In this paper we consider the problem of building a new class of metric maps representing the surroundings of a mobile robot moving in an unstructured indoor environment. Maps are conceived with a metric based on a log-polar space representation: this *retina-like* representation allows a better definition of objects near the robot, giving less importance to far ones. Information provided at each step by ultrasonic sensors has an uncertainty that is conceptualised as a fuzzy measure and is combined with previous data using Smets transferable believe model. The map building algorithm is integrated in a sensor-based robot navigation system able to recognise some characteristics of the environment. A pattern-matching algorithm, based on Mellin transform, takes advantage on the particular *retina-like* representation. Copyright ©2003 IFAC

Keywords: Fuzzy maps, fuzzy measures, localisation, robot navigation, log-polar.

## 1. INTRODUCTION

In recent years, the problem of indoor robot navigation has been largely considered and many researchers have worked out solutions able to perform complex navigation tasks in application fields ranging from industry to service robotics.

Choose the environment in a particular class, still very wide: an office like area with corridors, corners and other similar features. The navigation task to perform, described in linguistic terms containing topological elements such as *go straight along the corridor* or *turn right at first corner*, can be carried on using of a *topology-based* global map (Panzieri *et al.*, 2000) in which the structure and shape of the free-space is analysed and

connected components are classified as nodes of a graph using a semantic induced by the particular shape. Corridors or corners are then associated to nodes, and arcs are an adjacency relationship between these components. The high level planner can force a *navigation strategy* associating to the particular node a behavior that the mobile robot should bind to, while moving in that portion of the environment.

To efficiently implement this strategy a still open problem has to be solved: the devising of efficient strategies able to cope with the problem of *self localisation* in such unstructured environments, i.e., the ability of estimating the position of a mobile platform when no artificial landmarks can be used. *Natural* features, like shape of corridors

or lamps in the ceiling or even the number of encountered doors, have to be used and, obviously, the accuracy of such process must be sufficient to plan robot future actions. As a matter of fact, self localisation is always a multi-level process, usually consisting of more than one algorithm each one related to the accuracy requested for the subsequent motion steps. When covering large distances, motion accuracy along the path is not demanding and localisation can be more rough. On the contrary, when approaching the goal, this ability must be improved to allow fine motion. So, the global map must describe all the essential information being, at the same time, compact and easy to handle.

Suppose now that only low cost sonar sensors can be used: all localisation information, that at this point have a topological character, should be easily extracted from sensory data comparing the current sonar output with a set of reference signals associated with particular topological features. In most cases, association is done by comparing the current view with a static or dynamic list of models obtained with *a priori* considerations on the environment itself (Panzieri *et al.*, 2000; Micarelli *et al.*, 2000).

In particular, the problem we intend to address concerns the dynamic building of sonar-based digital images that can be use both for classification under one category belonging to a set of pre-determined topological situations (*corridor, corner, T-junction, end corridor, open space*), and for fine motion planning. The digital images here presented describe, in a log-polar metric, the surroundings of the mobile platform and then can be considered as metric local maps (see (Borenstein *et al.*, 1996)) updated at each navigation step.

In a dynamic environment, as for a robot navigating in an office-like space with people walking around, features (natural landmarks) necessarily vary and unknown configurations, due also to false reflections, have to be managed. This two-fold uncertainty pushes for a localisation algorithm that has to discriminate contradictory readings from changing landscapes just to fade planned actions or to ask, to the sensory system, an integration of actual data. To this aim, all the uncertainties deriving from the particular sensors used will be handled using the fuzzy measures theory (Klir and Folger, 1988).

## 2. UNCERTAINTY MODEL FOR ULTRASONIC RANGE FINDERS

Ultrasonic sensor performance may be rather poor due to various phenomena (Leonard and Durrant-Whyte, 1992) (multiple reflections, wide radiation

cone, etc.). As a consequence, the ultrasonic sensing process is affected by a large amount of uncertainty that is quite difficult to model. Should the sensors behave ideally, the synthesis of a bitmap of the free and the occupied space would present no conceptual difficulty. Unfortunately, this assumption is never verified in practice and, on the contrary, many mobile robot sensors are cheap units that are prone to several kinds of errors.

For illustration, we refer to the Polaroid Ultrasonic Rangefinder (Polaroid, 1987), a very common device that can detect distances in the range 0.12÷6.5 m with 1% accuracy. The multi-lobed power diagram of the transmitter may be obtained from the radiation directivity function of a plane circular piston

$$D(\vartheta) = 2 \frac{J_1(k\eta \sin \vartheta)}{k\eta \sin \vartheta}, \quad (1)$$

where  $J_1(\cdot)$  is the Bessel function of the first order,  $k = 2\pi/\ell$  depends on the wavelength  $\ell$ ,  $\eta$  is the piston radius and  $\vartheta$  is the azimuthal angle measured with respect to the beam central axis. For the Polaroid sensor it is  $\eta = 0.01921$  m and  $\ell = v/\varphi$ , where  $v$  is the sound speed in air and  $\varphi = 49.410$  kHz. In practice, it is sufficient to take into account only the principal lobe of the pattern, and consider the waves to be diffused over a radiation cone of  $25^\circ$  width.

A range reading  $r$  provides the information that one or more obstacles are located somewhere along the  $25^\circ$  arc of circumference of radius  $r$ . Hence, there is evidence that cells located in the proximity of this arc are ‘occupied’. On the other hand, cells well inside the circular sector of radius  $r$  are likely to be ‘empty’. To model this knowledge, we introduce the two functions

$$f_e(\rho, r) = \begin{cases} k_e & 0 \leq \rho < r - \Delta r \\ k_e \left(\frac{r-\rho}{\Delta r}\right)^2 & r - \Delta r \leq \rho < r \\ 0 & \rho \geq r, \end{cases} \quad (2)$$

$$f_o(\rho, r) = \begin{cases} 0 & 0 \leq \rho < r - \Delta r \\ k_o \left[1 - \left(\frac{r-\rho}{\Delta r}\right)^2\right] & r - \Delta r \leq \rho < r + \Delta r \\ 0 & \rho \geq r + \Delta r, \end{cases}$$

that describe, respectively, how the degrees of certainty of the assertions ‘empty’ and ‘occupied’ vary with the distance  $\rho$  of the cell  $c$  from the sensor, for a given range reading  $r$ . Here,  $k_e$  and  $k_o$  are two constants and  $2 \cdot \Delta r$  is the width of the area considered ‘proximal’ to the arc of radius  $r$  (see Fig. 1).

Since the intensity of the waves decreases to zero at the borders of the radiation cone, the degree of certainty of each assertion should be higher for cells close to the beam axis. This is realized by means of the following function

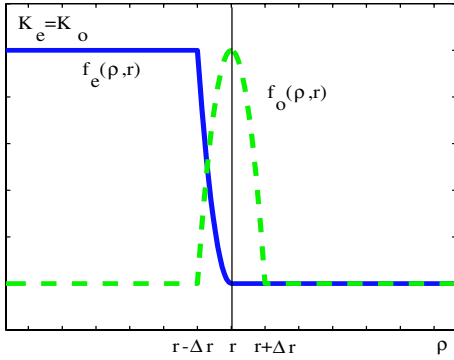


Fig. 1. Functions  $f_e$  and  $f_o$  relative to a range reading  $r$

$$f_a(\vartheta) = \begin{cases} D(\vartheta) & 0 \leq |\vartheta| \leq 12.5^\circ \\ 0 & |\vartheta| > 12.5^\circ, \end{cases} \quad (3)$$

where  $D(\vartheta)$  is the radiation directivity function (1).

Finally, a third function is introduced in order to weaken the confidence of each assertion as the distance from the sensor increases

$$f_d(\rho) = 1 - \frac{1 + \tanh(2(\rho - \rho_v))}{2}. \quad (4)$$

The parameter  $\rho_v$  plays the role of a ‘visibility radius’, i.e., a distance at which a smooth transition occurs from certainty to uncertainty.

For a better description of functions  $f_e$ ,  $f_o$ ,  $f_a$ ,  $f_d$  see (Oriolo *et al.*, 1997; Gambino *et al.*, 1997).

### 3. FUZZY MEASURES AND THE LOG-POLAR REPRESENTATION

Various approaches have been tried in the literature for the map building problem. Chronologically, the first has been the probabilistic approach which found its definitive formulation (Elfes, 1991) through the use of Bayesian techniques. To avoid some conceptual difficulties, some methodologies based on fuzzy logic have been successfully applied (Oriolo *et al.*, 1997). A third way to manage uncertainty, and here followed, is to use fuzzy measures theory (Klir and Folger, 1988; Gambino *et al.*, 1997) in conjunction with the Dempster-Shafer uncertainty calculus.

Consider a two-dimensional environment and assume that, for computational reasons, a discretised representation consisting in a set  $M$  of cells delimited by a log-polar grid can be adopted (see Fig. 2).

A series of range readings  $\{r_1, \dots, r_n\}$  collected at known sensor locations is available. In principle, the task of the Map Building System (MBS) should be to process the measures in order to determine, as accurately as possible, which cells are

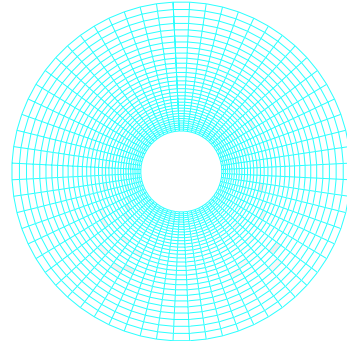


Fig. 2. log-polar grid

(even partially) occupied by obstacles and which cells are (completely) empty and thus suitable for robot navigation; no other characterisation of the cells is of interest. In fact, to build a classification algorithm able to recognise the shape of the surrounding environment, we are interested in estimating which cells are related to walls discriminating false reflections as well as unknown obstacles.

In view of this, to efficiently manage the degree of evidence available after a sensors reading and fusing it with previous ones, we make use of fuzzy measures theory (Klir and Folger, 1988).

Let  $U = \{o, e\}$  be the space of possible occupancy value (the universal set); then the power set of  $U$  is  $\mathcal{P}(U) = \{o, e, \{o, e\}, \emptyset\}$  and its elements represent, respectively, the values *occupied*, *empty*, *unknown*, *conflicting*.

For the application to ultrasonic map building, we must specify how the sensor readings are processed in order to obtain for each cell  $c$  of  $U$  the BPA. The first three functions of this assignment are  $m_e(c)$ , the degree of evidence that  $c$  is empty,  $m_o(c)$ , the degree of evidence that  $c$  is occupied, and  $m_{o,e}(c)$ , the degree of evidence that  $c$  is nothing more than a member of  $U$ .

In this paper, like in (Gambino *et al.*, 1997), we choose a basic probability assignment corresponding to a range reading  $r$  directly using the certainty functions (2–4)

$$m_e^r(c) = f_e(\rho, r) f_a(\vartheta) f_d(\rho), \quad (5)$$

$$m_o^r(c) = f_o(\rho, r) f_a(\vartheta) f_d(\rho), \quad (6)$$

$$m_{o,e}^r(c) = 1 - m_e^r - m_o^r, \quad m_\emptyset^r(c) = 0. \quad (7)$$

These assignments express the evidence that the cell  $c$ , whose centre is located at  $(\rho, \vartheta)$  belongs to the (crisp) sets  $\{e\}$ ,  $\{o\}$ ,  $\{o, e\}$  and  $\emptyset$ , respectively.

According to the standard Dempster rule of combination of two distinct and statistically independent pieces of evidence, that assumes a *closed-world* in which the possible states of a cell are only empty and occupied, the BPA should be updated letting the value of  $m_\emptyset(c)$  always zero. This is not

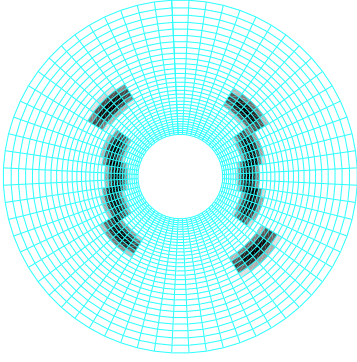


Fig. 3.  $m_o(c)$  before translation

our case, in which some contradiction can arise and, according to the navigation phase, has to be treated in a different way. To this aim, i.e., to combine several readings among them, the Smets rule (Smets, 1990a) will be used:

$$m_X^{1,2}(c) = \sum_{A \cap B = X} m_A^1(c) m_B^2(c), \quad \forall X \in \mathcal{P}(U). \quad (8)$$

The computation is initialised at  $m_\emptyset(c) = m_e(c) = m_o(c) = 0$  and  $m_{o,e}(c) = 1 \forall c \in M$ , i.e., *total ignorance*.

As an example, in Fig. 3 the mass distribution  $m_o$  obtained combining readings of 16 angularly equispaced sonar sensors in a corridor environment is reported.

#### 4. MAPPING DURING MOTION

A further and deeper analysis has to be devoted to the problem of map building after a motion phase. It is profitable, in fact, to take advantage of the amount of evidence that has been collected in a mass distribution relative to a certain robot position, after a translation of the robot itself. At least, it can be allowed a loose of the degree of evidence due both to the difficulty of such transformation involving a complex mapping of all the cells into smaller or bigger ones, and to real-time computation needs. Note that a simple rotation of the robot is not considered in this section. In fact, a rotation of the robot is only a change of the angular mapping of ultrasonic sensors and a change of the direction of motion w.r.t. the map itself: a rotation of the map is not effectively required.

Let say  $c$  and  $\hat{c}$  the cells of two log-polar maps centred at points  $P$  and  $\hat{P}$  respectively, and define as  $m_X(c)$  and  $\hat{m}_X(\hat{c})$ , with  $X \in \mathcal{P}(U)$ , the BMAs relative to those positions. Compute, for each cell  $\hat{c}_j$  with area  $A_j$  the area  $A_{j,i}$  of the intersection with each cell  $c_i$ ; obviously  $\sum_i A_{j,i} = A_j$ . Define now a crisp *interaction* function as

$$I(c_i, \hat{c}_j) = A_{j,i}/A_j \quad (9)$$

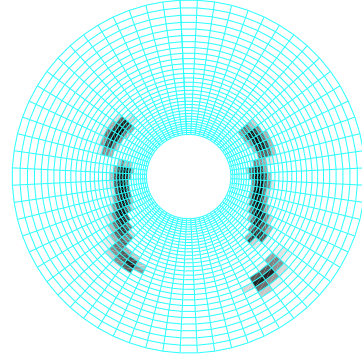


Fig. 4.  $m_o(c)$  after translation

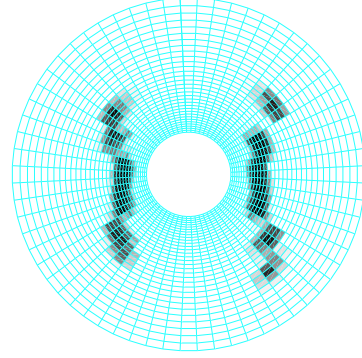


Fig. 5.  $m_o(c)$  after both translation and new sensor acquisition

that is eligible to represent how much the evidence accumulated in  $c_i$ , and stored in  $m_X(c_i)$  will influence the mass distribution  $\hat{m}_X(\hat{c}_j)$ . This transfer of belief can be done following a further consideration: we are not just translating the map, we are using its evidence to express a degree of belief in a proposition of the power set  $\mathcal{P}(U) = \{o, e, \{o, e\}, \emptyset\}$  related to a second map. To cope with this new belief a BMA  $\bar{m}_X(c)$  can be derived using the pignistic values (Smets, 1990b)  $BetP_o(c)$  and  $BetP_e(c)$ , with

$$BetP_X(c) = \sum_{B \subseteq \mathcal{P}(V)} m_X(c) \frac{|X \cap B|}{|B|}, \quad (10)$$

defining two auxiliary pignistic functions as

$$Pr_o(\hat{c}_j) = \sum_i I(c_i, \hat{c}_j) (BetP_o(c_i))$$

$$Pr_e(\hat{c}_j) = \sum_i I(c_i, \hat{c}_j) (BetP_e(c_i))$$

and assigning to the cells of the new map the following BMA.

$$\bar{m}_o(\hat{c}_j) = \begin{cases} Pr_o(c_i) - Pr_e(c_i) & \text{if positive} \\ 0 & \text{otherwise} \end{cases}$$

$$\bar{m}_e(c_j) = \begin{cases} Pr_e(c_i) - Pr_o(c_i) & \text{if positive} \\ 0 & \text{otherwise} \end{cases}$$

$$\bar{m}_{o,e}(\hat{c}_j) = 1 - \bar{m}_o(c_j) - \bar{m}_e(c_j)$$

$$\bar{m}_\emptyset(c_j) = 0.$$

Note that bets support only the winning proposition and the remaining mass is considered as unknown. In this way we do not generate contradiction during the translation phase and, conversely, we forget the contradiction mass of the old map. The mass of the empty set will arise again when fusing the sonar readings at the end of this phase. For cells that are not covered with this algorithm, representing the unexplored space, the BMA is obviously the *total ignorance* one.

This algorithm that we will define optimal requires the computation of the function  $I(c_i, \hat{c}_j)$  for each couple of cells of the two maps. A less demanding algorithm can be used to avoid the not-easy calculation of areas and intersections. This *sub-optimal* algorithm is carried on extracting from each cell  $c$ ,  $\bar{n}$  equally distributed points as representing samples of suitable percentage of its area (in our tests we set  $\bar{n} = 9$ ). Every test point has an assigned weight, which represent mean intersection rate between considered cell  $c$  and another cell  $c_j$ , whose  $c$  will be destination as consequence of traslation process. Then, each point of a cell is back-translated to locate its origin  $c_j$  and, as a first approximation, the whole area associated to the point is supposed to represent value  $I(c, c_j)$ , as the intersection between cells. The complexity of this reduced algorithm is  $O(\text{cell number} \times \bar{n})$ .

The result of a translation of 30 cm of the map showed in Fig. 3, obtained with this second algorithm, is reported in Fig. 4. After merging new sensor readings in this map, the mass distributions  $m_o(c)$  become the one reported in Fig. 5. Note that walls are becoming more coherent because conflicting measures are going to support the  $m_\emptyset(s)$  distribution.

After this combination phase we are ready to extract from the mass distribution the digital images that best fit to our navigation tasks. For example, if we want to compute a navigation map ( $\mathcal{NM}$ ) suitable for a safe path planning, i.e., in the free space, we can compute the degree of plausibility of *not empty* cell:

$$Pl_{\bar{e}}(c) = Bel_{o,e} - Bel_e(c) = 1 - m_e(c), \quad (11)$$

this is the maximum amount of potential specific support that can be given to the proposition *not empty*. Note that, the last equality is computed under the assumption that the mass of the empty set  $m_\emptyset(c)$  is dropped into  $m_{o,e}(c)$ , recovering the hypothesis of *closed word*, i.e., a cell can be only free or occupied. This map is reported in Fig. 6.

On the other hand, to the purpose of the recognition of the actual feature, a log-polar Local Map ( $\mathcal{LM}$ ) can be computed as the result of a binarization, by means of an appropriate threshold, of the navigation map ( $\mathcal{NM}$ ). Note that a centring

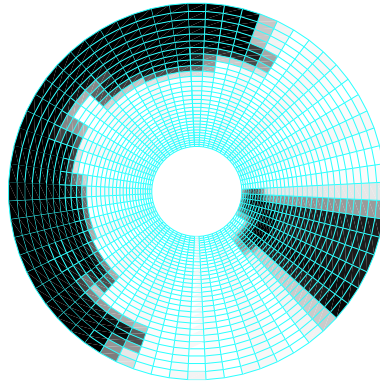


Fig. 6.  $\mathcal{NM}$  during navigation

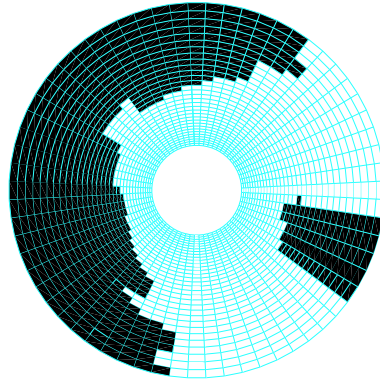


Fig. 7.  $\mathcal{LM}$  of a corner

procedure is also performed on the navigation map  $\mathcal{NM}$  to make more reliable the recognition phase that will be described in the next section.

## 5. ROBOT SELF LOCALISATION

The robot localisation phase, following the approach presented in (Panzieri *et al.*, 2000), can be divided into two main steps: the first one consisting in computing a similarity function giving a degree of evidence about the shape of the surrounding environment (*static recognition*), and a second one able to merge evidences coming from sensors readings related to different time instants and/or robot positions (*dynamic recognition*).

For the *static recognition* phase several pattern matching methods can be applied. A promising one, based on Mellin transform, will be presented in this section. A Mellin transform of a bi-dimensional surface is, by definition, a bi-dimensional Fourier transform after a log-polar coordinate transformation. Being the  $\mathcal{LM}$  already a log-polar discretised mapping with  $2^5 \times 2^6$  values, a simple bi-dimensional Fast Fourier Transform (FFT2) will deliver the required Mellin transform. This operator is invariant w.r.t. rotating and scaling operations and therefore particularly useful in pattern matching algorithms for environments that can appear rotated or scaled compared with their reference models. Cause Mellin operator is

not invariant w.r.t. translating operations and, at the same time, the number of provided patterns is restricted to essential one, it's necessary to translate  $\mathcal{LM}$ , before applying Mellin operator, for a better pattern matching. So it's useful to compute a log-polar coordinates couple  $(\rho, \theta)$ , called *centre of navigation*, which is positioned on the mean axis, connecting the nearest visible obstacles for a couple of opposite sensors. Then  $\mathcal{LM}$  is translated to centre digitalized map respect of *centre of navigation*.

For the *dynamic recognition* phase the approach followed is based again on the use of the Transferable Belief Model of Smets (Smets, 1990a) with a universe of discourse (the reference set) defined by  $\Omega = \{\text{corridor, corner, T-junction, end corridor, open space}\}$  and a basic mass assignment derived by the similarity function  $R(L)$ , with  $L \in \Omega$ , previously defined.

Let  $F$  be an element of  $P(\Omega)$ , the power set of  $\Omega$ . At each step, a BMA  $m_F^R$  is determined: this function quantifies how much the event  $F$  is supported by the available information. In our case the available information consists of the similarity values calculated in the static recognition phase. A possible BMA can be obtained using the decision tree depicted in Fig. 8: a unitary mass is assigned to the root, i.e., the unknown proposition, and a splitting algorithm, based on the similarity values, is used, when possible, to drop the mass towards the leaves of the tree. At each step, as shown in Fig. 8, a different similarity is used and the percentage of mass dropped to the winning subtree is determined taking into account its ability to discriminate the particular feature. If the mass is under a threshold no dropping is applied and the BMA is stopped. At each navigation step the BMA obtained is used to update the mass distribution of  $P(\Omega)$  with Smets rule.

Now, following (Smets, 1990b), the pignistic transformation  $BetP_X$ , can be used to take a decisions and deduce which hypothesis is the best one.

## REFERENCES

Borenstein, J., Everett, H.R. and Feng, L., *Navigating mobile robot: sensors and techniques*, A. K. Peters, Ltd., Wellesley, MA, 1996.

Panzieri, S., Petroselli, D., Ulivi, G., "Topological localization on indoor sonar based fuzzy maps," In: Pagello E, Groen F, Arai T, Dillmann R, Stentz A (eds) *Intelligent Autonomous System 6*, IOS Press, Amsterdam, NL, pp 596-603, 2000.

Fabrizi, E. and Saffiotti, A., "Extracting topology-based maps from gridmaps", *Proc. of Int.*

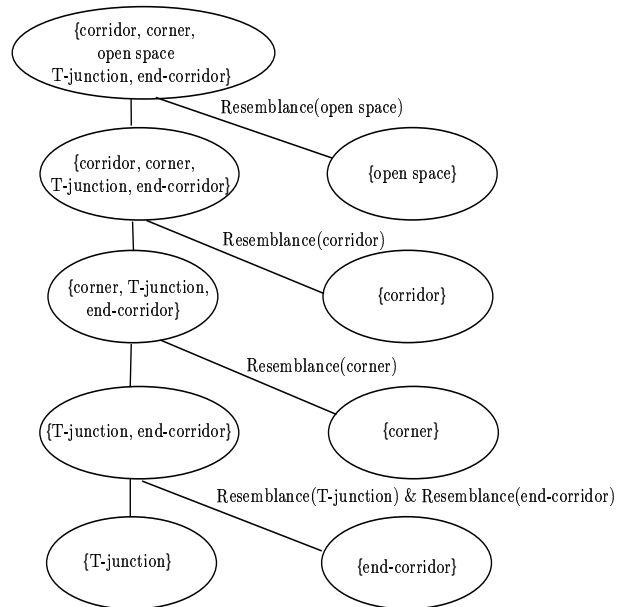


Fig. 8. Decision tree

*Conf. on Robotics and Automation*, San Francisco, CA, 2000.

Oriolo, Ulivi, G. and, Vendittelli, M., "Fuzzy Maps: A New Tool for Mobile Robot Perception and Planning," *Journal of Robotic Systems*, **14**(3), pp. 179-197, 1997.

Gambino, F., Ulivi, G. and Vendittelli, M., "The Transferable Belief Model in Ultrasonic Map Building," *IEEE Int. Conf. on Fuzzy Systems*, pp. 601-608, Barcelona, ES, 1997.

J. J. Leonard and H. F. Durrant-Whyte, *Directed Sonar Sensing for Mobile Robot Navigation*. Kluwer Academic Publishers, 1992.

G. J. Klir and T. A. Folger, *Fuzzy sets*. Kluwer Academic Publishers, 1988.

A. Elfes, "Occupancy grids: A stochastic spatial representation for active robot perception," in *Autonomous Mobile Robots: Perception, Mapping, and Navigation* ( S. S. Iyengar and A. Elfes, eds.), IEEE Computer Society Press, pp. 60-71, 1991.

Polaroid Corporation, "Ultrasonic Ranging System", 1987.

P. Smets, "The combination of evidence in the transferable believe model," *IEEE Trans. on Pattern Analysis and Machine Intelligence*, vol. 12, n. 5, pp. 447-458, 1990.

P. Smets, "Constructing the pignistic probability function in a context of uncertainty," in *Uncertainty in Artificial Intelligence* ( M. Enrion, R.D. Shacter, L.N. Kanal, and J.F. Lemmere, eds.), North Holland, Amsterdam, pp. 29-39, 1990.

A. Micarelli, A. Neri, S. Panzieri, G. Sansonetti, "A case-based approach to indoor navigation using sonar maps," 6th Int. IFAC Symp. On Robot Control, pp. 345-350, Vienna, Austria, 2000.